

The Large Helical Device: Entering Deuterium Experiment Phase Toward Steady-State Helical Fusion Reactor Based on Achievements in Hydrogen Experiment Phase

Yasuhiko Takeiri¹

Abstract—The large helical device (LHD) is one of the world's largest superconducting helical system fusion-experiment devices. Since the start of experiments in 1998, LHD has extended its parameter regime, aiming at achievement of the reactor-relevant plasma conditions and the exploration of related plasma physics in helical-type magnetic configurations. The LHD has also demonstrated its inherent advantage for steady-state operation. Based on these leading developments of helical plasma research, LHD has progressed to the advanced research phase, that is, the deuterium experiment that started in March 2017. It is expected that plasma parameters should be extended toward more reactor-relevant regime, and the related physics research is allowed in such extended regime. Taking this opportunity, parameter extensions such as density, temperature, and steady-state operation achieved in the hydrogen experiment phase are overviewed, along with the initial highlighted results in the very first deuterium experiment campaign in 2017. The design activity of LHD-type steady-state helical fusion reactor is also briefly introduced.

Index Terms—Large helical device (LHD), deuterium experiment, high-beta (β) plasmas, high-temperature plasmas, plasma heating devices, parameter extension, FFHR-d1.

I. INTRODUCTION

HIGH-PERFORMANCE and steady-state plasmas are required to realize fusion reactor. The large helical device (LHD) [1], one of the largest magnetically confined fusion experimental devices, has pursued this goal based on heliotron concept [2]. Heliotron concept is categorized as a helical system. Helical systems in general have inherent advantage in regard to steady-state operation.

The principal device dimensions are height: ~ 9 m, diameter: ~ 13 m, and the mass: ~ 1500 t. Experiment started in March 1998, and LHD has conducted pioneering research since then. After a long period of technical and administrative arrange-

Manuscript received October 12, 2017; revised December 7, 2017; accepted December 12, 2017. Date of publication January 9, 2018; date of current version July 9, 2018. The review of this paper was arranged by Senior Editor S. J. Gitomer.

The author is with the National Institute for Fusion Science, National Institutes of Natural Sciences, Graduate University for Advanced Studies, Toki 509-5292, Japan (e-mail: takeiri@nifs.ac.jp).

Color versions of one or more of the figures in this paper are available online at <http://ieeexplore.ieee.org>.

Digital Object Identifier 10.1109/TPS.2017.2784380

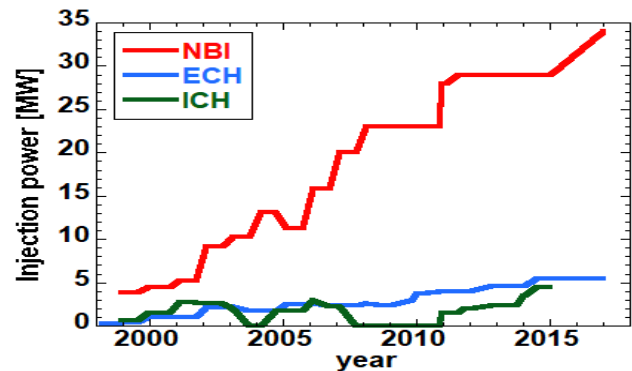


Fig. 1. History of plasma heating powers in LHD experiment.

ments, LHD has just entered the advanced stage of research by exploiting the deuterium plasmas from March 7, 2017 [3].

LHD is equipped with three kinds of heating systems, neutral beam injection (NBI) [4], electron cyclotron heating (ECH) [5], and ion cyclotron heating (ICH) [6]. These heating powers have been steadily increased as shown in Fig. 1, to provide parameter extensions of LHD plasmas associated with many new physics findings.

In this review paper, such parameter extensions achieved in the hydrogen experiment phase are briefly reviewed with emphasis on associated physics findings. Initial highlighted results obtained in the very first campaign of the deuterium experiment will be briefly mentioned (details will be reported in upcoming separate papers). Progress toward steady-state helical fusion reactor, based on the heliotron concept, is also briefly introduced.

II. OVERVIEW OF PARAMETER EXTENSION ACHIEVED IN HYDROGEN EXPERIMENT PHASE

In this section, achievements in LHD during the hydrogen experiment phase are briefly overviewed, with emphasis on its parameter extensions.

A. Steady Buildup of Heating Systems

The heating power has been steadily increased as shown in Fig. 1, and has reached the total injection power of NBI: 34 MW, ECH: 5.5 MW, and ICH: 3 MW, respectively.

The NBI system is composed of five beam lines. Three of them are negative-ion-based beams with the nominal energy of 180 keV (16 MW in total in hydrogen beams and about the half of it for deuterium beams), and the other two are positive-ion-based ones with the nominal energy and power of 40 keV and 6 MW/each (60 and 80 keV both with 9 MW) for hydrogen (deuterium) beams [7].

The ECH system consists of three 77-GHz, and two 154-GHz gyrotrons which contribute to the fundamental and second-harmonic resonance heating at 2.75 T, respectively. The former can also be used at 1.375 T as the second-harmonic resonance heating, as well.

As for ICH, all the ICH antennas are now temporarily removed for smooth initiation of deuterium experiment, although they had been playing crucial roles to explore long-pulse operation [8] in hydrogen experiment phase. They will be reinstalled in the near future for conducting steady-state operation in deuterium plasmas.

B. Extensions of Density and Temperature in Hydrogen Experiment Phase

As one of the highlights in parameter extensions in hydrogen experiment phase of the LHD, extensions of temperature and density are reviewed in this section.

In the initial phase of the LHD experiment, high electron temperature (T_e) plasma production was mainly conducted by means of high-energy NBI (~ 180 keV) and ECH, in which the electron internal transport barrier (ITB) formation was found and investigated in detail as in [9]. The electron-root radial electric field [10] is observed in the core region of such high T_e plasmas with much higher than the ion temperature, T_i . Based on this peculiar nature commonly observed in other helical devices such as CHS [11], W7-AS [12], and TJ-II [13], plasmas with predominant core electron heating producing the steep T_e gradient with the positive radial electric field are also known as core electron-root confinement (CERC) [14]. The T_e exceeded 20 keV (in the density range of a few 10^{18} m^{-3}) in the hydrogen experiment phase.

The demonstration of the one of the fusion conditions, that is, the ion temperature of 10 keV, is one of the missions in LHD [15]. NBIs with low energy (~ 40 keV) were installed one by one (fourth and fifth beamlines) to increase the direct ion heating power. The T_i was gradually increased, along which the ion-ITB formation was found and studied in detail [16], [17]. The scenario optimization such as wall conditioning for reducing recycling effectively worked for high- T_i plasma production [17] through the increase of the ion heating in the core region. The highest T_i in the hydrogen experiment phase was 8.1 keV. It should be also noted that so-called impurity hole [16] was found in high- T_i plasmas. A hollow profile of carbon density was observed associated with the increase of core T_i , in contrast to the electron density profile. This finding has led to the detailed investigation for the density profiles of different plasma species in order to elucidate that density profiles of carbon and helium ions are hollow while the bulk hydrogen ion is peaked [18].

The efforts to achieve simultaneous high temperatures of both electron and ion also have been made. Superposition of

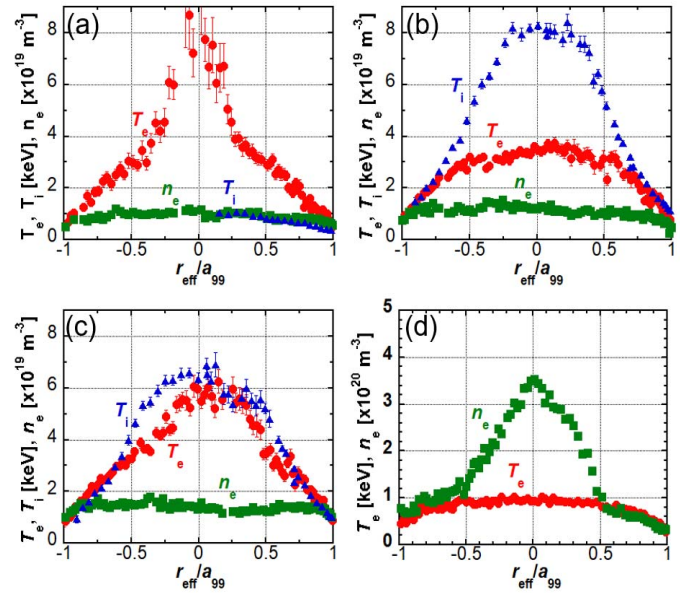


Fig. 2. Typical density and temperature profiles of (a) electron ITB (CERC), (b) ion ITB, (c) simultaneous high temperatures, and (d) superdense core plasmas. The injected power for each case (ECH, NBI) is (a) (3.2, 2.75), (b) (0, 24.7), (c) (2.2, 20.2), and (d) (0, 11.5), respectively.

ECH power with the range of 5 MW onto the high- T_i plasmas produced the plasma with T_i and T_e of about 7.5 and 6 keV, simultaneously [19].

The plasma production with the density beyond the equivalent tokamak density limit [20] was also one of the highlights in the hydrogen experiment phase in the LHD. This is called as superdense core (SDC) [21] plasma associated with the internal diffusion barrier (IDB) formation. Repetitive pellet injection [22] in outer-shifted magnetic configurations (in which MHD stability properties are favorable) produced the IDB with particle diffusion coefficient as low as less than 0.1 m^2/s [23]. This finding has provided the new scenario with high-density/low-temperature core plasma in the future helical fusion reactor [24].

Typical density and temperature profiles of electron ITB, ion ITB, simultaneous high temperatures, and superdense core plasmas are shown together in Fig. 2, and the operational regime on the (T_i and T_e) plane in Fig. 3.

C. High- β Plasma Production and Its Strategy

As for high- β plasma production, we have intensively explored several magnetic configurations with varying vacuum magnetic axis positions for current free, that is, disruption-free plasmas. Fig. 4 shows strategies for high- β plasma production in hydrogen experiment phase in LHD, which is summarized in the plane of the central β value (β_0), and the magnetic axis position (R_{ax}) (not the vacuum ones). Data are categorized to four different vacuum magnetic axis positions, 3.6 m (hatched in light green), 3.65 m (light orange), 3.75 m (light blue), and 3.85 m (light purple).

There have been two scenarios. One is the standard scenario based on broad pressure profile, and the other is based on the discovery of SDC [21] with peaked pressure profile. The

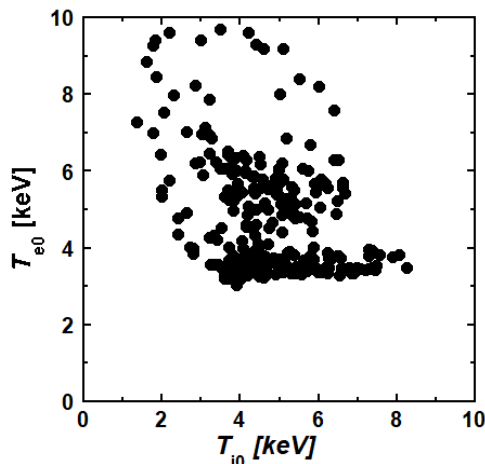


Fig. 3. Temperature regime for the hydrogen experiment phase plotted on central values of T_i and T_e .

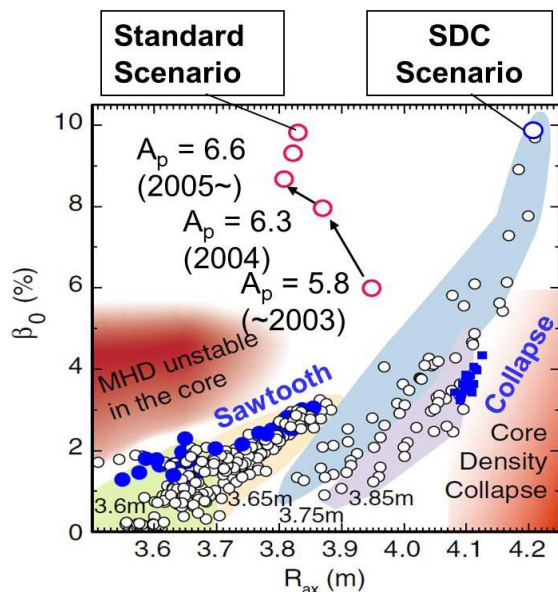


Fig. 4. Operation regime of high- β plasmas in the hydrogen experiment phase in LHD, on the plane of central β value (β_0), and the magnetic axis position (R_{ax}). Legends are as follows. Black open symbol: no event, blue circle: sawtooth event, blue square: core density collapse, red open circle: history of raising β_0 values in standard scenario, and blue open circle: the highest β_0 value achieved in SDC scenario.

record value of volume-averaged β of 5.1% was achieved in the standard scenario.

The inward-shifted configurations have better heating efficiency, which is attributed to better particle confinement property. Standard scenario employs the broad pressure profile (gas puffing or a single pellet injection) to make the magnetic axis shift smaller to secure better heating efficiency. The MHD unstable (Sawtooth event) in the core region (indicated in Fig. 4) was found to be the obstacle to further raise the β value, and the magnetic configurations with higher aspect ratio (A_p) were employed based on their smaller magnetic axis shift. This kind of scenario optimization has led to the

increase of β beyond the MHD unstable in the core region, and achieved β of 5.1% at the magnetic field strength, B , of 0.425 T (corresponding to the data in red with β_0 of around 10%).

On the other hand, SDC scenario (high density ($>10^{20} \text{ m}^{-3}$) with the peaked pressure profile by means of multiple pellet injection) employs magnetic configuration with the vacuum magnetic axis position of 3.75 m and beyond, which can overcome MHD instability in the core region. However, in this case, core density collapse [25] was found to be the obstacle. Careful tailoring of discharge scenario successfully led to β_0 of around 10%, as shown in the top right in Fig. 4.

In both cases, collisionality in produced high- β plasmas is relatively high (such as by the low temperature in standard scenario with $B = 0.425 \text{ T}$ and high density in SDC scenario). Thus, study on high- β plasmas in low-collisional regime is necessary toward more reactor-relevant research. In this regard, high- β trials have been extensively conducted in recent years at configurations with $B = 1 \text{ T}$ with inward-shifted magnetic axis position in order to increase the temperature with better NBI heating efficiency. As reported in [26], we have achieved the volume-averaged β of 3.4% in quasi-steady state for gas puffing and 4.1% for multiple pellet injections.

In such a way, high- β operational regime has been extended to lower collisional regime at higher magnetic field strength than before.

D. World-Record Steady-State Operation Achieved in Hydrogen Experiment Phase

It is well known that helical systems have the advantage of steady-state operation since they do not need to run plasma current to form the magnetic field for plasma confinement. LHD has steadily demonstrated this, by resolving several difficult issues such as thermal treatment and damage control with continuous large heat flux on the divertor plates, the real-time feedback control with several time scales (density and heating power) [27], impurity influx associated with plasma heating sources, the unintended entrance of the exfoliated mixed-material layers caused by continuous divertor erosion [28], and others.

Integration of high-power steady-state heating devices [29], plasma operation, and the modification of divertor have led to the world-record steady-state operation, as shown in Fig. 5. The plasma density and temperatures (ion and electron) are about $1.2 \times 10^{19} \text{ m}^{-3}$ and 2 keV, respectively [Fig. 5(a) and (b)]. The pulse duration was 2859 s ($\sim 47 \text{ min } 39 \text{ s}$) with about 1.2-MW heating power (ECH: 0.26 MW and ICH: 0.94 MW), which resulted in the world-record total injected energy to the plasma, 3.36 GJ, in the fusion experiment. This value is beyond the record values in tokamak (Tore Supra) [30].

Feedback operation scheme worked effectively such as the boosting RF power dealing with the rapid increase in the density [as recognized at ~ 500 and $\sim 1400 \text{ s}$, Fig. 5(a), (c), and (d)], and continuous He fuelling [Fig. 5(a)].

Fig. 6 (reproduced and modified from [31]) shows the achieved fusion triple product as a function of the duration of plasma discharge, in comparison among tokamaks

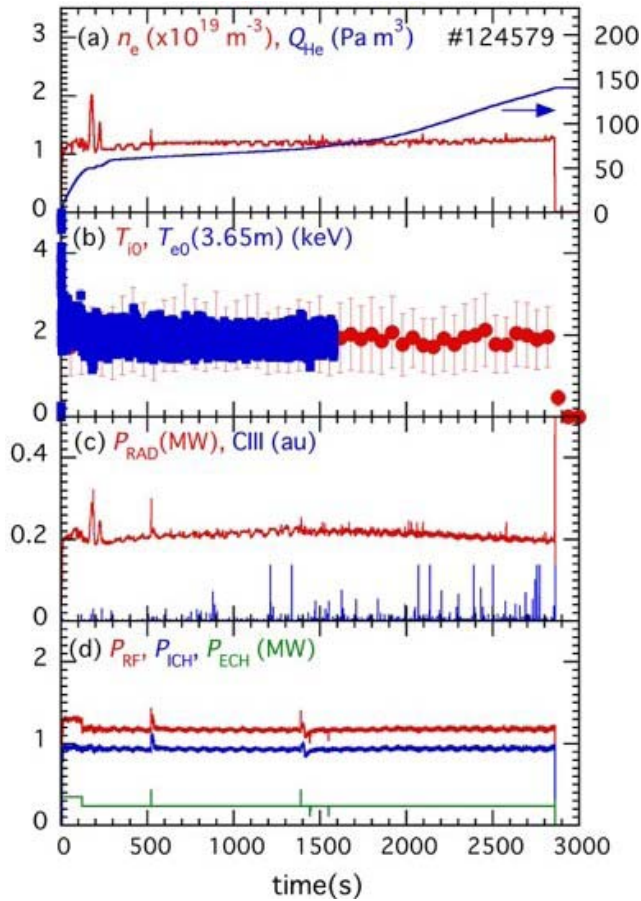


Fig. 5. Waveforms of the ultralong (2859 s) discharge. (a) Line-averaged electron density and the He fueling. (b) Ion and electron temperatures. (c) Total radiation power and line intensity of carbon spectrum. (d) Heating power. Modified from [27, Fig. 2].

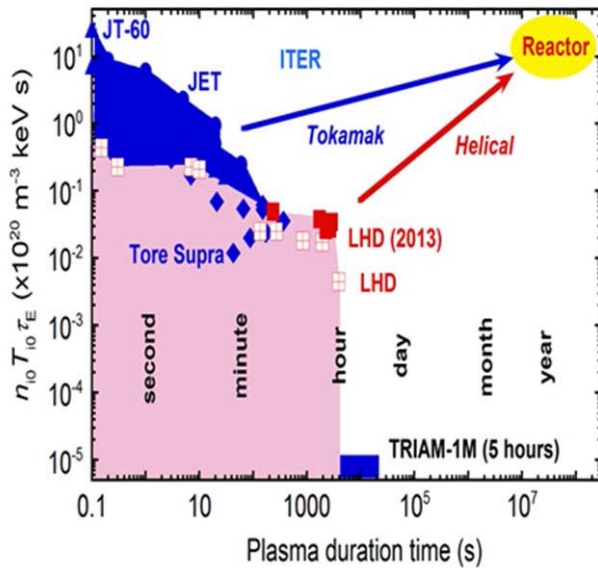


Fig. 6. Achieved fusion triple product as a function of the duration of the plasma discharge.

and LHD. It is worthwhile to note that the ATF stellarator produced steady-state plasma with pulselength greater than 1-h (~ 4667 s) with zero plasma current and modest plasma

parameters (density of $\sim 0.3 \times 10^{19} \text{ m}^{-3}$ for 70-kW ECH power) [32]. As for tokamaks, TRIAM-1M achieved 5-h discharge with the electron density $< 0.1 \times 10^{19} \text{ m}^{-3}$ and the lower hybrid heating power of ~ 0.05 MW [33]. Other than this, the envelope of tokamak experiments consists of break-even experiment in JT-60U, and steady-state operations in Tore Supra. Although the data points in LHD have reached hour range as described here, further improvement for higher performance (fusion triple product) is required. In tokamaks, further improvement in steady-state operation is demanded, although fusion triple product had reached break-even condition. Complementary research among helical systems and tokamaks are envisaged toward steady-state high-performance reactor regime.

Integration of these individually achieved parameters should be pursued for designing core plasma scenario for steady-state helical fusion reactor.

III. HIGHLIGHTS OF THE FIRST CAMPAIGN OF LHD DEUTERIUM EXPERIMENT (IN BRIEF)

LHD has started the deuterium plasma experiment on March 7, 2017. The main objectives of the deuterium experiment are as follows:

- 1) high-performance plasmas through confinement improvement;
- 2) clarification of the isotope effect on confinement;
- 3) the demonstration of the confinement capability of energetic ions in heliotron magnetic configuration;
- 4) plasma-wall interaction or plasma-material interaction (PMI) study in deuterium plasmas.

Achievement of T_i of 10 keV [34] is the most highlighted result, which should be the milestone of the helical system research demonstrating its capability for satisfying one of the fusion conditions and providing the firm prospects toward the helical fusion reactor.

It was found that ECH-heated plasmas with almost the same T_e (about 10 keV) and the same electron density ($1.5 \times 10^{19} \text{ m}^{-3}$ at core) can be produced by less ECH power in deuterium plasmas than in hydrogen plasmas. T_i at core region is about 1.5 and 1 keV for this specific set of deuterium and hydrogen plasma. This is the same tendency which has been predicted by linear gyrokinetic trapped electron mode simulation [35].

Neutron emission rate measurement has made quantitative argument possible, such as on the plasma confinement property depending on the magnetic configurations [36], [37] and on the interaction between MHD modes and energetic particles confinement [38], [39].

Triton burn-up ratio was evaluated for the first time in helical systems. It reflects the confinement capability of decelerated tritons produced from D–D fusion reactions. The clear dependence of the triton burn-up ratio on the magnetic configurations was recognized (better for inward-shifted configurations and larger magnetic field strength). The highest burn-up ratio so far measured is 0.45% [36].

Wide-ranging studies such as the energy confinement [40]–[42], carbon impurity behavior [43], divertor plasma [44], and plasma response to resonant magnetic

perturbation [45] have been intensively conducted in deuterium plasmas through the comparison with those in hydrogen plasmas. These on-going studies should accomplish above mentioned objectives systematically.

IV. CONCEPTUAL DESIGN OF THE LHD-TYPE STEADY-STATE FUSION REACTOR, FFHR-D1, BASED ON LHD EXPERIMENTS

The conceptual design of the LHD-type steady-state helical fusion reactor, FFHR-d1 [46], has been intensively conducted based on close collaboration with LHD experiment and numerical simulations.

A self-consistent steady-state operation point with the energy multiplication factor $Q \sim 10$ has been searched to provide a concrete scenario for burning plasma operation in such a reactor. Such operation point has been identified by fulfilling several criteria self-consistently as shown in [47], where three conditions are employed. The first condition is the ratio of the turbulent transport level to the neoclassical transport level, the second condition is Mercier index, D_I [48], for one of the measures for the MHD stability, and the third condition is the fusion gain (Q value). These evaluations are now relatively easily possible by the established numerical suite including the empirical (direct profile extrapolation [49] approach based on actual LHD discharges) 1-D transport solver and numerical codes for 3-D magnetic configurations (equilibrium, neoclassical transport, and others, being utilized and validated against LHD discharges) [47]. Of course, there are more and more criteria from both physics and engineering points of view, and the systems code, HELIOSCOPE [50], manages this kind of iterative process to identify and grasp the relevant operation point or regime.

Quantitative assessment for startup scenario reaching such an identified operation point has also progressed. Control algorithm such as of the auxiliary heating power and the fueling amount has also been examined to reach the identified operation point [47]. In this way, conceptual design of the LHD-type steady-state helical fusion reactor, FFHR-d1, has been progressing.

V. CONCLUSION

LHD has steadily extended its parameter regime in its hydrogen experiment phase, highlighted such as by (separately achieved, though) the electron temperature above 20 keV, the ion temperature of 8.1 keV, the density far above the density limit in equivalent tokamak, the volume-averaged β value of 5.1%, and steady-state plasma discharge for about 48 min with the world record of the total injected energy of 3.36 GJ. The steady increase of the heating power provided these progresses along with the physics findings such as the ITB formation and impurity hole formation.

LHD has progressed to the advanced research phase, that is, the deuterium experiment which began in March 2017. Achievement of T_i of 10 keV is one of the highlighted results in the very first campaign of the deuterium experiment, which is the milestone of the helical system research demonstrating its capability for satisfying one of the fusion conditions and

providing the firm prospects toward helical fusion reactor. For establishing a firm basis for designing a steady-state helical fusion reactor, wide-ranging research has been intensively conducted such as on isotope effect, confinement capability of energetic particles through direct measurement of fusion-produced neutrons, plasma-material interactions, and others.

Conceptual design of the LHD-type steady-state helical fusion reactor has also been progressing based on all these progresses in LHD. Further progress anticipated in the deuterium experiment will be reflected in such design activity.

ACKNOWLEDGMENT

The author would like to thank all the domestic and international collaborators for their extensive cooperation. The LHD experiment and all of the NIFS activities have been continuously and strongly supported by the Ministry of Education, Culture, Sports, Science and Technology, Japan, and domestic and international collaborators.

REFERENCES

- [1] Y. Takeiri *et al.*, "Extension of the operational regime of the LHD towards a deuterium experiment," *Nucl. Fusion*, vol. 57, no. 10, p. 102023, 2017.
- [2] K. Uo, "The confinement of plasma by the heliotron magnetic field," *J. Phys. Soc. Jpn.*, vol. 16, pp. 1380–1395, Feb. 1961.
- [3] Y. Takeiri, "Prospect towards steady-state helical fusion reactor based on progress of LHD project entering the deuterium experiment phase," *IEEE Trans. Plasma Sci.*, to be published.
- [4] Y. Takeiri *et al.*, "High performance of neutral beam injectors for extension of LHD operational regime," *Fusion Sci. Technol.*, vol. 58, no. 1, pp. 482–488, 2010.
- [5] T. Shimozuma *et al.*, "ECRH-related technologies for high-power and steady-state operation in LHD," *Fusion Sci. Technol.*, vol. 58, no. 1, pp. 530–538, 2010.
- [6] T. Mutoh *et al.*, "ICRF heating system in LHD," *Fusion Sci. Technol.*, vol. 58, no. 1, pp. 504–514, 2010.
- [7] M. Osakabe *et al.*, "Preparation and commissioning for the LHD deuterium experiment," *IEEE Trans. Plasma Sci.*, to be published.
- [8] T. Mutoh *et al.*, "Steady-state operation and high energy particle production of MeV energy in the large helical device," *Nucl. Fusion*, vol. 47, no. 9, pp. 1250–1257, 2007.
- [9] K. Ida *et al.*, "Characteristics of electron heat transport of plasma with an electron internal-transport barrier in the large helical device," *Phys. Rev. Lett.*, vol. 91, no. 8, p. 085003, 2003.
- [10] L. M. Kovrizhnykh, "Neoclassical theory of transport processes in toroidal magnetic confinement systems, with emphasis on non-axisymmetric configurations," *Nucl. Fusion*, vol. 24, no. 7, pp. 851–936, 1984.
- [11] A. Fujisawa *et al.*, "Electron thermal transport barrier and density fluctuation reduction in a toroidal helical plasma," *Phys. Rev. Lett.*, vol. 82, no. 13, pp. 2669–2672, 1999.
- [12] H. Maaßberg, C. D. Beidler, U. Gasparino, M. Romé, and W.-A. Team, "The neoclassical 'electron root' feature in the Wendelstein-7-AS stellarator," *Phys. Plasmas*, vol. 7, no. 1, pp. 295–311, 2000.
- [13] F. Castejón *et al.*, "Enhanced heat confinement in the flexible heliac TJ-II," *Nucl. Fusion*, vol. 42, no. 3, pp. 271–280, 2002.
- [14] M. Yokoyama *et al.*, "Core electron-root confinement (CERC) in helical plasmas," *Nucl. Fusion*, vol. 47, no. 9, pp. 1213–1219, 2007.
- [15] A. Iiyoshi, M. Fujiwara, O. Motojima, N. Ohyabu, and K. Yamazaki, "Design study for the large helical device," *Fusion Sci. Technol.*, vol. 17, no. 1, pp. 169–187, 1990.
- [16] K. Ida *et al.*, "Observation of an impurity hole in a plasma with an ion internal transport barrier in the large helical device," *Phys. Plasmas*, vol. 16, no. 5, p. 056111, 2009.
- [17] K. Nagaoka *et al.*, "Integrated discharge scenario for high-temperature helical plasma in LHD," *Nucl. Fusion*, vol. 55, no. 11, p. 113020, 2015.
- [18] A. Perek *et al.*, "Observation of the bulk ion density peaking in a discharge with an impurity hole in the LHD," *Nucl. Fusion*, vol. 57, no. 7, p. 076040, 2017.

- [19] H. Takahashi *et al.*, “Extension of operational regime in high-temperature plasmas and effect of ECRH on ion thermal transport in the LHD,” *Nucl. Fusion*, vol. 57, no. 8, p. 086029, 2017.
- [20] H. Yamada, “Complementary study,” in *Proc. AIP Conf.*, 2008, pp. 178–198.
- [21] N. Ohya *et al.*, “Observation of stable superdense core plasmas in the large helical device,” *Phys. Rev. Lett.*, vol. 97, no. 5, p. 055002, 2006.
- [22] R. Sakamoto *et al.*, “Impact of pellet injection on extension of the operational region in LHD,” *Nucl. Fusion*, vol. 41, no. 4, pp. 381–386, 2001.
- [23] R. Sakamoto *et al.*, “Pellet injection and internal diffusion barrier formation in large helical device,” *Plasma Fusion Res.*, vol. 2, p. 047, 2007.
- [24] O. Mitarai, A. Sagara, R. Sakamoto, N. Ohya, A. Komori, and O. Motojima, “High-density, low temperature ignited operations in FFHR,” *Plasma Fusion Res.*, vol. 5, p. S1001, 2010.
- [25] H. Yamada *et al.*, “Characterization and operational regime of high density plasmas with internal diffusion barrier observed in the large helical device,” *Nucl. Fusion*, vol. 49, no. 12B, pp. B487–B496, 2007.
- [26] S. Sakakibara *et al.*, “Extension of high-beta plasma operation to low collisional regime,” presented at the 26th IAEA Fusion Energy Conf., Kyoto, Japan, Oct. 2016, paper EX/4-4.
- [27] H. Kasahara, Y. Yoshimura, K. Nagasaki, M. Tokitani, N. Ashikawa, “Progress of high-performance steady-state plasma and critical PWI issue in LHD,” presented at the 25th IAEA Fusion Energy Conf., St. Petersburg, Russia, Oct. 2014, paper EX/3-4.
- [28] M. Tokitani *et al.*, “Plasma wall interaction in long-pulse helium discharge in LHD—Microscopic modification of the wall surface and its impact on particle balance and impurity generation,” *J. Nucl. Mater.*, vol. 463, pp. 91–98, Aug. 2015.
- [29] H. Kasahara *et al.*, “Development of steady-state operation using ion cyclotron heating in the large helical device,” *Phys. Plasmas*, vol. 21, no. 6, p. 061505, 2014.
- [30] D. van Houtte *et al.*, “Recent fully non-inductive operation results in Tore Supra with 6 min, 1 GJ plasma discharges,” *Nucl. Fusion*, vol. 44, no. 5, pp. L11–L15, 2004.
- [31] M. Kikuchi and M. Azumi, *Frontiers in Fusion Research II*. Switzerland: Springer, 2015.
- [32] T. C. Jernigan *et al.*, “Long pulse experiments on the advanced toroidal facility,” *Phys. Plasmas*, vol. 2, no. 6, pp. 2435–2439, 1995.
- [33] S. Itoh *et al.*, “Recent progress in the superconducting tokamak TRIAM-1M,” *Nucl. Fusion*, vol. 39, no. 3A, pp. 1257–1270, 1999.
- [34] H. Takahashi *et al.*, “Confinement characteristics of ion ITB plasmas with deuterium in the LHD,” presented at the 21st Int. Stellarator-Heliotron Workshop, Kyoto, Japan, Oct. 2017, p. I-22.
- [35] M. Nakata, M. Nunami, H. Sugama, and T.-H. Watanabe, “Isotope effects on trapped-electron-mode driven turbulence and zonal flows in helical and tokamak plasmas,” *Phys. Rev. Lett.*, vol. 118, no. 16, p. 165002, 2017.
- [36] M. Isobe *et al.*, “Neutron diagnostics in the large helical device,” *IEEE Trans. Plasma Sci.*, to be published.
- [37] S. Murakami *et al.*, “Studies of energetic beam ion confinement and neutron production rates in the deuterium plasma of LHD,” presented at the 21st Int. Stellarator-Heliotron Workshop, Kyoto, Japan, Oct. 2017, p. P2-49.
- [38] S. Ohdachi *et al.*, “Energetic particle driven resistive interchange mode in the deuterium LHD experiments,” presented at the 21st Int. Stellarator-Heliotron Workshop, Kyoto, Japan, Oct. 2017, p. I-23.
- [39] K. Ogawa *et al.*, “Enhancement of radial transport of energetic ion by helically-trapped energetic-ion driven resistive interchange mode in LHD,” presented at the 21st Int. Stellarator-Heliotron Workshop, Kyoto, Japan, Oct. 2017, p. PD-1.
- [40] H. Yamada *et al.*, “Energy confinement and thermal transport properties of dimensionally similar NBI-heated plasmas with hydrogen and deuterium on LHD,” presented at the 21st Int. Stellarator-Heliotron Workshop, Kyoto, Japan, Oct. 2017, p. P2-45.
- [41] K. Tanaka *et al.*, “Isotope effects on transport and turbulence in LHD,” presented at the 21st Int. Stellarator-Heliotron Workshop, Kyoto, Japan, Oct. 2017, p. P2-46.
- [42] F. Warmer *et al.*, “Energy confinement of hydrogen and deuterium electron-root plasmas in the large helical device,” presented at the 21st Int. Stellarator-Heliotron Workshop, Kyoto, Japan, Oct. 2017, p. P2-51.
- [43] K. Mukai *et al.*, “Carbon impurities behaviour of high-ion-temperature discharges with deuterium in the large helical device,” presented at the 21st Int. Stellarator-Heliotron Workshop, Kyoto, Japan, Oct. 2017, pp. 2–32.
- [44] S. Masuzaki *et al.*, “Comparison of the divertor plasma properties between H and D discharges in the large helical device,” presented at the 21st Int. Stellarator-Heliotron Workshop, Kyoto, Japan, Oct. 2017.
- [45] Y. Narushima *et al.*, “Study of plasma response of magnetic island produced by resonant magnetic perturbation in LHD deuterium plasmas,” presented at the 21st Int. Stellarator-Heliotron Workshop, Kyoto, Japan, Oct. 2017, p. P1-26.
- [46] A. Sagara *et al.*, “Helical reactor design FFHR-d1 and c1 for steady-state DEMO,” *Fusion Eng. Des.*, vol. 89, nos. 9–10, pp. 2114–2120, 2014.
- [47] T. Goto *et al.*, “Development of a real-time simulation tool towards self-consistent scenario of plasma start-up and sustainment on helical fusion reactor FFHR-d1,” *Nucl. Fusion*, vol. 57, no. 6, p. 066011, 2017.
- [48] A. Glasser, J. M. Greene, and J. L. Johnson, “Resistive instabilities in general toroidal plasma configurations,” *Phys. Fluids*, vol. 18, no. 7, pp. 875–888, 1975.
- [49] J. Miyazawa, “Direct extrapolation of radial profile data to a self-ignited fusion reactor based on the gyro-Bohm model,” *Fusion Eng. Des.*, vol. 86, no. 12, pp. 2879–2885, 2011.
- [50] T. Goto *et al.*, “Design window analysis for the helical DEMO reactor FFHR-d1,” *Plasma Fusion Res.*, vol. 7, p. 2405084, 2012.

Authors’ photographs and biographies not available at the time of publication.